Adaptive CSP for user independence in MI-BCI paradigm for upper limb stroke rehabilitation

Costa, Ana P.; Møller, Jakob Skadkær; Iversen, Helle K.; Puthusserypady, Sadasivan

Published in:
Proceedings of GlobalSIP 2018

Publication date:
2019

Document Version
Publisher's PDF, also known as Version of record

ADAPTIVE CSP FOR USER INDEPENDENCE IN MI-BCI PARADIGM FOR UPPER LIMB STROKE REHABILITATION

Ana P. Costa, Jakob S. Møller, Helle K. Iversen and Sadasivan Puthusserypady

***Abstract*—A 3-class motor imagery (MI) Brain-Computer Interface (BCI) system, that implements subject adaptation with short to non-existing calibration sessions is proposed. The proposed adaptive common spatial patterns (ACSP) algorithm was tested on two datasets (an open source data set (4-class MI), and an in-house data set (3-class MI)). Results show that when long calibration data is available, the ACSP performs only slightly better (4%) than the CSP, but for short calibration sessions, the ACSP significantly improved the performance (up to 4-fold). An investigation into class separability of the in-house data set was performed and was concluded that the "Pinch"movement was more easily discriminated than "Grasp" and "Elbow Flexion". The proposed paradigm proved feasible and provided insights to help choose the motor tasks leading to best results in potential real-life applications. The ACSP enabled a successful semi user independent scenario and showed potential to be a tool towards an improved, personalized stroke rehabilitation protocol.**

***Index Terms*—Brain-computer interface (BCI), Stroke rehabilitation, Sensorimotor rhythms (SMR), Adaptive Common Spatial Patterns (ACSP)**

I. Introduction

Brain-Computer Interface (BCI) technology allows for brain signals to be recorded and translated into output commands, which can be used in various applications. In electroencephalogram (EEG) setups, sensorimotor rhythms (SMRs) are some of the signals of interest which can be measured. SMRs are tuned by motor intentions, such as motor imagery (MI), and are characterized by a modulation of the amplitudes of the measured electrical potentials.

One area where MI-BCI systems have real-world applications is in neuro-rehabilitation, namely in stroke cases. Current stroke rehabilitation therapies present some limitations [1]–[3] and different enhancing strategies are emerging, of which BCIs are a promising one [4]. Rehabilitative BCIs aim at exploiting brain plasticity to improve motor recovery in patients. MI is used in most studies for this purpose, as it is hypothesized that it promotes neuroplasticity-related repair of the damaged brain areas [5]. The basis of MI-BCI systems for stroke rehabilitation has been laid by studies reporting an increase in motor cortex excitability as well as topographical changes after training [6]. Preliminary results such as [7], [8] indicate the feasibility of incorporating BCI in post-stroke hand rehabilitation. Nevertheless, more large, randomized clinical trials are necessary to confirm the advantages and reliability of the method.

Another issue to consider, is that individual stroke characteristics lead to different consequent neuroplastic changes during recovery, which indicates that an ideal system should be tailored for each patient [9]. This is related to one of the disadvantages of many BCI systems, which is subject-dependence: systems require data from a long training session for each subject, where no feedback is given to the user. This is impractical and particularly undesirable in the context of stroke rehabilitation, where it is important that the patients start receiving feedback as soon as possible.

A. Adaptive Spatial Filters

A commonly used strategy for source localization in MI-BCI systems is the common spatial pattern (CSP) filters. However, it presents some setbacks, namely that (i) it requires large data to avoid overfitting and generate robust projecting vectors, while being quite sensitive to outliers and (ii) it is typically subject-dependent and has no ability to adapt to the non-stationarities that are characteristic of EEG signals [10]. These characteristics imply that long subject-dependent calibration sessions are needed for computing the filter coefficients. Therefore, variations of the algorithm are needed to solve these problems and improve its performance. There are two ways to incorporate new data in order to handle changes that occur between distinct EEGs: block-wise [10], [11] and sample-wise. Here, a Recursive Least Squares (RLS) approach was implemented for sample-wise adaptation of the CSP filter, similar to the method used by [12] for the axDAWN filter.

II. Materials and Methods

A. Signal Processing

1) The CSP Filter: Let $\mathbf{X}_j \in \mathbb{R}^{C_n \times N}$ be the j^{th} EEG trial, where N is the number of samples/trial and C_n is the number of channels. Then, the filtered trial $\mathbf{Z}_{j,CSP} \in \mathbb{R}^{C_n \times N} = \mathbf{W}\,\mathbf{X}_j$, where $\mathbf{W} \in \mathbb{R}^{C_n \times C_n}$ is the matrix parameterizing the signal decomposition. Here, we denote each column $(\mathbf{w}_{i,i=1,2,\ldots,C_n})$ of $\mathbf{W}$ as a spatial filter, and each column of $\mathbf{W}^{-1}$ as a spatial pattern. The normalized covariance matrix for class k is defined as:

$$\mathbf{C}_k = \frac{1}{T_n}\sum_{j=1}^{T_n}\frac{\mathbf{X}_{j(k)}\mathbf{X}_{j(k)}^T}{\text{trace}\{\mathbf{X}_{j(k)}\mathbf{X}_{j(k)}^T\}}, \tag{1}$$

where T_n is the number of trials, $\mathbf{X}_{j(k)}$ is the j^{th} trial belonging to class $k \in [1, K]$ and $K = 2$ for the binary classification case, which we will use, for simplicity, to explain

the algorithm. In [13], the CSP is described with a discriminative view, which was useful to derive the ACSP. Considering $\mathbf{C}_d = \mathbf{C}_1 - \mathbf{C}_2$ and $\mathbf{C}_c = \mathbf{C}_1 + \mathbf{C}_2$ as the discriminative activity ($\mathbf{C}_d$), *i.e.* the band-power modulation between the two classes, and the common activity ($\mathbf{C}_c$), the solution to the following maximization problem can be achieved by solving the GED problem:

$$\underset{\mathbf{W}}{\operatorname{argmax}} \frac{\mathbf{W}^T\mathbf{C}_d\mathbf{W}}{\mathbf{W}^T\mathbf{C}_c\mathbf{W}}. \tag{2}$$

A One-Versus-All (OVA) multiclass version of the CSP was used so that the algorithm can be used to distinguish between more than two classes [14]. Finally, to get a system that is trainable on a small amount of data, the CSP was regularized with Diagonal Loading (DLCSP algorithm) [15].

2) Adaptive Spatial Filter (ACSP): A sample-wise adaptive approach to the CSP algorithm based on the RLS method for GED is introduced here [16]. A training set is used to initialize the CSP matrix. Expanding Eq.(2), it can be deducted that:

$$\underset{\mathbf{W}}{\operatorname{argmax}} \frac{\mathbf{W}^T\mathbf{C}_d\mathbf{W}}{\mathbf{W}^T\mathbf{C}_c\mathbf{W}} = \underset{\mathbf{W}}{\operatorname{argmax}} \frac{\mathbf{W}^T\mathbf{C}_1\mathbf{W}}{\mathbf{W}^T\mathbf{C}_c\mathbf{W}}. \tag{3}$$

Both $\mathbf{C}_1$ and $\mathbf{C}_c$ represent full normalized covariance matrices of stationary signals with zero mean. Rearranging the solution to the GED problem as in [16], we obtain the basis for the iterative algorithm:

$$\mathbf{W} = \frac{\mathbf{W}^T\mathbf{C}_c\mathbf{W}}{\mathbf{W}^T\mathbf{C}_1\mathbf{W}}\mathbf{C}_c^{-1}\mathbf{C}_1\mathbf{W}. \tag{4}$$

A temporal discrete variable n is now introduced and an estimate of the primal eigenvector $\mathbf{w}_1(n)$ is computed as:

$$\hat{\mathbf{w}}_1(n) = \frac{\mathbf{w}_1^T(n')\mathbf{C}_c(n)\mathbf{w}_1(n')}{\mathbf{w}_1^T(n')\mathbf{C}_1(n)\mathbf{w}_1(n')}\mathbf{C}_c^1(n)^{-1}\mathbf{C}_1^1(n)\mathbf{w}_1(n') \tag{5}$$

where $n' = n - 1$. Some comments about Eq.(5):

1) *Iterative computation of class covariance matrices:* Here, we have not prioritized an asynchronous, self-paced system which results in an advantage for the development of the ACSP, specifically in this step, because we always know the true label of each sample $\mathbf{x}(n)$. Therefore, we can iteratively update the normalized $\mathbf{C}_1(n)$ only when $\mathbf{x}(n) \in class1$, while $\mathbf{C}_c(n)$ is always updated:

$$\begin{aligned}\mathbf{C}_1(n) &= \mathbf{C}_1(n') + \frac{\mathbf{x}_1(n)\mathbf{x}_1^T(n)}{\text{trace}\{\mathbf{x}_1(n)\mathbf{x}_1^T(n)\}} \text{ and} \\ \mathbf{C}_c(n) &= \mathbf{C}_c(n') + \frac{\mathbf{x}(n)\mathbf{x}^T(n)}{\text{trace}\{\mathbf{x}(n)\mathbf{x}^T(n)\}},\end{aligned} \tag{6}$$

where $\mathbf{x}(n)$ is any data sample taken at time n and $\mathbf{x}_1(n)$ represents the data belonging only to class 1.

2) *Iterative computation of the inverse of* $\mathbf{C}_c(n)$*:* This step in Eq.(5) would imply a very high computational effort which is not feasible for an online application. Therefore, as in [12], [16], the Sherman-Morrison-Woodbury formula is used for the iterative update of $\mathbf{C}_c^{-1}(n)$ [17]:

$$\mathbf{C}_c^{-1}(n) = \mathbf{C}_c^{-1}(n') - \frac{\mathbf{C}_c^{-1}(n')\mathbf{x}(n)\mathbf{x}^T(n)\mathbf{C}_c^{-1}(n')}{1 + \mathbf{x}^T(n)\mathbf{C}_c^{-1}(n')\mathbf{x}(n)}. \tag{7}$$

It is advantageous to use Eq.(7) since only $\mathbf{C}_c^{-1}(n')$ needs to be stored and only simple matrix operations are required for each iteration. Finally, a deflation technique [16] is used to iteratively estimate the remaining eigenvectors ($\mathbf{w}_i$'s).

$$\begin{aligned}\mathbf{C}_1^i(n) &= \left[\mathbf{I} - \frac{\mathbf{C}_1^{i-1}(n)\mathbf{w}_{i-1}(n)\mathbf{w}_{i-1}^T(n)}{\mathbf{w}_{i-1}^T(n)\mathbf{C}_1^{i-1}(n)\mathbf{w}_{i-1}(n)}\right]\mathbf{C}_1^{i-1}(n), \\ \mathbf{C}_c^i(n) &= \mathbf{C}_1^{i-1}(n).\end{aligned} \tag{8}$$

To compute $\mathbf{w}_i'$s, Eq.(5) is used with the respective $\mathbf{C}_1^i(n)$ and $\mathbf{C}_c^i(n)$ computed as in Eq.(8). As in [12], the $\mathbf{w}_i'$s are normalized for numerical reasons.

$$\mathbf{w}_i(n) = \frac{\hat{\mathbf{w}}_i(n)}{[\hat{\mathbf{w}}_i^T(n)\mathbf{C}_c^i(n)\hat{\mathbf{w}}_i(n)]^{\frac{1}{2}}}. \tag{9}$$

After all the spatial filters of trial n have been computed, the first and last m vectors are stored to classify trial $n + 1$.

3) Classification Algorithm: Discriminant Analysis (DA) was the chosen method to perform the classification, due to its low computational complexity and comparable performances to more complex approaches [12], [18], [19]. To overcome some of the limitations of DA, Friedman's regularized version of DA [20] (RDA) was implemented [21].

B. Dataset Description and Experimental Design

1) Dataset 1: 4-class MI of different body parts: This dataset belongs to the BCI competition IV [22] (dataset 2a) and comprises of the EEG recordings on 9 subjects of four classes of MI from distinct body parts (left and right hand, feet and tongue). For each subject, two sessions of 288 trials were recorded, namely a calibration session without feedback and an evaluation session with feedback.

2) Dataset 2: 3-class MI of single upper limb: This dataset was recorded in our laboratory and was obtained in two different days: a short calibration session recorded without feedback and a longer session with feedback. The three motor tasks (Fig. 1) were performed with the right arm. A goal-oriented visual interface was implemented, as it has been proven to improve classification results [18]. For the calibration day, each session of MI consisted of 6 runs of 18 trials. Each trial started with a warning sound and a fixation cross, for the subject to mentally prepare for the task (2 seconds). Then, it was replaced by a visual cue indicating which of the three motor tasks the subject should imagine (4 seconds). Finally, the screen became blank and the subject could rest (2 seconds). In the online session, a vertical green bar positioned on the right side of each cue displayed real-time feedback (the bar grew from bottom to top, one fragment at a time for correct classifications). The user started receiving feedback after 1 second.

The recordings were done on 14 healthy subjects aged between 20-31. The subjects were sitting comfortably in a chair placed approximately one meter from the screen displaying the visual interface. During the experiment, the subjects

(a) (b) (c)

Fig. 1. Visual interface of the BCI system. (a) Palmar grasp (Class 1) - engaging all fingers and palm to hold an imaginary object between them. (b) Pinch (Class 2) - collecting the fingertips of the thumb, index and middle finger. (c) Elbow Flexion (Class 3) - flexing the elbow while maintaining the wrist aligned with the arm, with the thumb directed upwards/towards the subject as the forearm is lifted.

placed their right hand comfortably on the table in front of them and kept all movements to a minimum. 16 active Ag/AgCl electrodes were used spanning the motor cortex area. All procedures involving human subjects were performed in accordance to the ethical standards of the 1964 Helsinki declaration and of the national research committee.

C. Data Analysis Setup

Before analysis, the data was band-pass (7-30 Hz) filtered using a 4^{th} order zero-phase Butterworth filter. Two distinct strategies were used to asses the performance of the ACSP filter on dataset 1: (1) *User dependent strategy:* one CSP filter and RDA classifier were trained for each subject using all the data from the calibration session and tested on the evaluation data, and (2) *Semi user independent strategy:* shorter calibration sessions were used to initialize the feature extraction and classification parameters. This allows for potential customization of the BCI system for the individual needs of each patient. After testing the ACSP on dataset 1, it was used on dataset 2, where the training size was short and determined based on the previous results.

III. Results and Discussion

A. Dataset 1: 4-class MI of different body parts

1) User dependent strategy: An investigation of the convergence of the adaptive filter was made prior to the analysis of the classification performances. In Table I, the classification performances of the CSP and ACSP in the unseen evaluation data are displayed and compared to the results of the winning algorithm (filter bank CSP (FBCSP)) of the BCI competition [14], with the best performance for each subject highlighted in bold. While a one-sided paired t-test indicated that the difference between the performance of the FBCSP and that of the ACSP algorithm was non-significant (p-value of 0.141 at a confidence level of $\alpha = 0.05$), the first still outperformed the latter in all subjects except three. A similar paired t-test revealed that there is no significant difference between the CSP and the ACSP ($p = 0.294$). These results indicate that there is little advantage in using the ACSP algorithm when sufficient training data is available. Finally, the scalp topographies were analyzed and it was concluded that the ACSP lead to physiologically significant patterns similar to the ones obtained by the regular CSP algorithm.

TABLE I
Classification Performance (as Maximum Kappa Value) of ACSP, CSP and the Winner (FBCSP) of the BCI Competition IV in the Unseen Evaluation Data of Dataset 1.

Subjects	CSP	ACSP	FBCSP [14]
1	0.677	**0.683**	0.676
2	0.363	0.231	**0.417**
3	0.602	0.677	**0.745**
4	0.465	0.377	**0.481**
5	0.246	0.330	**0.398**
6	0.243	**0.366**	0.273
7	0.612	0.568	**0.773**
8	0.749	0.704	**0.755**
9	0.565	**0.771**	0.606
Mean	0.502	0.523	**0.569**
Median	0.565	0.568	**0.606**

2) Semi user independent strategy: In this approach, the number of trials per class was made to vary from 15 to 65 in steps of 15 and the resulting kappa values corresponding to the classification performances on the evaluation dataset were calculated for each case. The trials chosen for each class were taken randomly. The result is presented in Fig. 2. It is clear

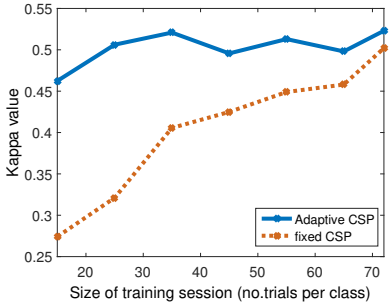

Fig. 2. Evolution of classification performance on evaluation dataset for different sizes on the training session (online simulation). Samples of growing size from the calibration dataset were used to train the CSP, for each subject, and evaluated on the corresponding evaluation dataset, using the same procedure as in section III-A1. The average maximum kappa value of all subjects is used as evaluation performance.

that the performance of the CSP decreases significantly with smaller training sizes. The ACSP, however, results in kappa values similar to the final one already from a very small set. While the difference in performance kappa between algorithms for a training size of 72 is only 0.021, for a training size of 35 the difference is 0.115. This represents a 1.28-fold increase. Based on this analysis, the training sizes for dataset 2 were chosen to be 36.

B. Dataset 2: 3-class MI of single upper limb

A similar convergence analysis was made for dataset 2 and it indicated convergence around 17 trials per class. In Table II, the classification performances obtained during the online feedback session in terms of average maximum kappa values for the MI are summarized. We conclude that the

TABLE II
PERFORMANCES FROM THE MI ONLINE SESSION OF DATASET 2 WITH REAL TIME FEEDBACK GIVEN AS AVERAGE MAXIMUM KAPPA VALUE.

Subjects		1	2	4	5	6	7	8	9	10	11	12	13	14	**Mean**	**Median**
DLCSP	Fixed	0.10	0.08	0.05	0.19	0.05	0.10	0.08	0.05	0.21	0.05	0.30	0.13	0.08	0.11	0.08
	Adaptive	**0.36**	**0.49**	**0.52**	**0.46**	**0.49**	**0.65**	**0.50**	**0.71**	**0.651**	**0.48**	**0.33**	**0.33**	**0.22**	**0.47**	**0.49**

ACSP resulted in a 4-fold increase in performance of the DLCSP, which is a significant result ($p = 5 \times 10^{-5}$). The performance of the ACSP is comparable with the literature for similar problems [18], [23]. Finally, an investigation into class separability was made, by extracting and combining the binary confusion matrices for each class (Table III). The results suggest that class 2 (Pinch) was the easiest to discriminate, and class 3 (Elbow Flexion) the hardest.

TABLE III
CLASSIFICATION PERFORMANCES FOR PAIRWISE CLASS DISCRIMINATION, FOR THE ONLINE FEEDBACK SESSION.

Class combination	1 vs 2	1 vs 3	2 vs 3
Kappa value	0.632	0.516	0.579

IV. CONCLUSION

The feasibility of a 3-class MI-BCI paradigm which could be employed for enhancement to the current stroke rehabilitation therapies has been studied. The RLS-based ACSP seems to overcome one of the main disadvantages of the CSP filter, allowing for personalized training programs based on short calibration sessions. The ACSP provided only slightly better results than the CSP when there was plenty training data, but performed up to 4 times better when not. The classification performances are lower in the second dataset, confirming that it is a harder task to distinguish between motor tasks performed by the same limb. An investigation on the separability of the chosen motor tasks indicates that the "Pinch" movement was the easiest to discriminate, which can suggest a direction for class choice in future similar studies. The system here implemented could be a step towards a potential application of MI-BCI technology for enhancement of current post-stroke neuro-rehabilitation. Overall, there is still room for improvement towards practical applicability, such as channel reduction and development of an unsupervised version of the algorithm. Large and randomized clinical trials are also necessary to confirm the advantages and reliability of the method.

REFERENCES

[1] B. Ovbiagele and M. Nguyen-Huynh, "Stroke epidemiology: Advancing our understanding of disease mechanism and therapy," *Neurotherapeutics*, vol. 8, pp. 319–329, Jul. 2011.

[2] D. Mozaffarian, E. J. Benjamin, A. S. Go, D. K. Arnett, M. J. Blaha, M. Cushman, S. R. Das, S. de Ferranti, J.-P. Després, H. J. Fullerton *et al.*, "Heart disease and stroke statistics 2016 update: a report from the american heart association," *Circulation*, vol. 133, no. 4, pp. e38–e360, 2016.

[3] V. Gadidi, M. Katz-Leurer, E. Carmeli, and N. Bornstein, "Long-term outcome post stroke: predictors of activity limitation and participation restriction." *Arch. Phys. Med. Rehabil.*, vol. 92, no. 11, pp. 1802–1808, Nov. 2011.

[4] U. Chaudhary, N. Birbaumer, and A. Ramos-Murguialday, "Brain-computer interfaces for communication and rehabilitation," *Nat. Rev. Neurol.*, vol. 12, no. 9, pp. 513–525, Sep. 2016.

[5] W. Teo and E. Chew, "Is motor-imagery brain-computer interface feasible in stroke rehabilitation?" *PM. R.*, vol. 6, no. 8, pp. 723–728, Aug. 2014.

[6] U. Chaudhary, N. Birbaumer, and M. R. Curado, "Brain-machine interface (BMI) in paralysis," *Ann. Phys. Rehabil. Med.*, vol. 58, no. 1, pp. 9–13, 2015.

[7] A. Ramos-Murguialday, D. Broetz, M. Rea, L. Laer, O. Yilmaz, F. Brasil, G. Liberati, M. Curado, E. Garcia-Cossio, A. Vyziotis, W. Cho, M. Agostini, E. Soares, S. Soekadar, A. Caria, L. Cohen, and N. Birbaumer, "Brain-machine interface in chronic stroke rehabilitation: A controlled study," *Ann. Neurol.*, vol. 74, no. 1, pp. 100–108, Jul. 2013.

[8] K. K. Ang, C. Guan, K. S. Phua, C. Wang, L. Zhou, K. Y. Tang, G. J. Ephraim Joseph, C. W. Keong Kuah, and K. S. Geok Chua, "Brain-computer interface-based robotic end effector system for wrist and hand rehabilitation: Results of a three-armed randomized controlled trial for chronic stroke," *Front. Neuroeng.*, vol. 7, p. 30, 2014.

[9] D. J. Leamy, J. Kocijan, K. Domijan, J. Duffin, R. A. Roche, S. Commins, R. Collins, and T. E. Ward, "An exploration of EEG features during recovery following stroke–implications for BCI-mediated neurorehabilitation therapy," *J. Neuro. Rehabil.*, vol. 11, no. 1, p. 9, 2014.

[10] X. Song and S. Yoon, "Improving brain-computer interface classification using adaptive common spatial patterns," *Comput. Biol. Med.*, vol. 61, no. 6, pp. 150–160, Jun. 2015.

[11] V. Mondini, A. L. Mangia, and A. Cappello, "EEG-based BCI system using adaptive features extraction and classification procedures," *Comp. Intell. Neurosci.*, vol. 2016, p. 4562601, 2016.

[12] H. Woehrle, M. M. Krell, S. Straube, S. K. Kim, E. A. Kirchner, and F. Kirchner, "An adaptive spatial filter for user-independent single trial detection of event-related potentials," *IEEE Trans. Biomed. Eng.*, vol. 62, no. 7, pp. 1696–1705, 2015.

[13] B. Blankertz, R. Tomioka, S. Lemm, M. Kawanabe, and K. R. Müller, "Optimizing spatial filters for robust EEG single-trial analysis," *IEEE Sig. Proc. Mag.*, vol. 25, no. 1, pp. 41–56, Dec. 2008.

[14] K. K. Ang, Z. Y. Chin, C. Wang, C. Guan, and H. Zhang, "Filter bank common spatial pattern algorithm on BCI competition iv datasets 2a and 2b," *Front. Neurosci.*, vol. 6, p. Article 39, 2012.

[15] F. Lotte and C. Guan, "Regularizing Common Spatial Patterns to Improve BCI Designs: Unified Theory and New Algorithms," *IEEE Trans. Biomed. Eng.*, vol. 58, no. 2, pp. 355–62, Feb. 2010.

[16] Y. Rao and J. Principe, "An RLS type algorithm for generalized eigendecomposition," *Neur. Net. Sig. Proc.*, pp. 263–272, 2001.

[17] G. H. Golub and C. F. Van Loan, *Matrix computations*. John Hopkins University Press,, 2013.

[18] X. Yong and C. Menon, "EEG classification of different imaginary movements within the same limb," *PLoS ONE*, vol. 10, pp. 1–24, 2015.

[19] F. Lotte, M. Congedo, A. Lécuyer, F. Lamarche, and B. Arnaldi, "A review of classification algorithms for EEG-based brain–computer interfaces," *J. Neural Eng.*, vol. 4, no. 2, p. R1, 2007.

[20] J. H. Friedman, "Regularized discriminant analysis," *J. Amer. Stat. Assoc.*, vol. 84, no. 405, pp. 165–175, 1989.

[21] A. Schloegl and C. Brunner, "Biosig: A free and open source software library for BCI research," *Computer*, vol. 41, no. 10, pp. 44–50, 2008.

[22] M. Tangermann, K.-R. Mueller, A. Aertsen, N. Birbaumer, C. Braun, C. Brunner, R. Leeb, C. Mehring, K. J. Miller, G. R. Mueller-Putz, G. Nolte, G. Pfurtscheller, H. Preissl, G. Schalk, A. Schoegl, C. Vidaurre, S. Waldert, and B. Blankertz, "Review of the BCI competition iv," *Front. Neurosci.*, vol. 6, no. 7, p. 55, 2012.

[23] M. Jochumsen, I. Niazi, K. Dremstrup, and E. Kamavuako, "Detecting and classifying three different hand movement types through electroencephalography recordings for neurorehabilitation," *Med. Biol. Eng. Comput.*, vol. 54, no. 10, pp. 1491–1501, Oct. 2016.